Annu. Rev. Biomed. Eng. 2000. 02:477–509
Copyright © 2000 by Annual Reviews. All rights reserved

BIOPHYSICAL INJURY MECHANISMS IN ELECTRICAL SHOCK TRAUMA

Raphael C. Lee, Dajun Zhang, and Jurgen Hannig
Department of Surgery and Organismal Biology (Biomechanics), Pritzker School of Medicine, The University of Chicago, Chicago, Illinois 60637; e-mail: rlee@surgery.bsd.uchicago.edu

Annu. Rev. Biomed. Eng. 2000.2:477-509. Downloaded from arjournals.annualreviews.org
by UNIVERSITY OF CHICAGO LIBRARIES on 10/02/06. For personal use only.

Key Words electrical injury, burn, membrane, electroporation, denaturation, tissue

■ **Abstract** Electrical shock trauma tends to produce a very complex pattern of injury, mainly because of the multiple modes of frequency-dependent tissue-field interactions. Historically, Joule heating was thought to be the only cause of electrical injuries to tissue by commercial-frequency electrical shocks. In the last 15 years, biomedical engineering research has improved the understanding of the underlying biophysical injury mechanisms. Besides thermal burns secondary to Joule heating, permeabilization of cell membranes and direct electroconformational denaturation of macromolecules such as proteins have also been identified as tissue-damage mechanisms. This review summarizes the physics of tissue injury caused by contact with commercial-frequency power lines, as well as exposure to lightning and radio frequency (RF), microwave, and ionizing radiation. In addition, we describe the anatomic patterns of the resultant tissue injury from these modes of electromagnetic exposures.

CONTENTS

1523-9829/00/0825-0477$14.00

INTRODUCTION

No area of technical advance has had a greater impact on human culture than electrical power. Tools of modern human society are increasingly electrical-power driven owing to the ease of power transmission and efficiency of electromechanical and electrochemical energy conversion. However, as convenient as it is, high-power electrical circuits also present a constant threat to society, especially young children, electricians, construction workers, and home improvement fanatics. Almost everyone has, at least once in his or her lifetime, been shocked by electricity. The fear reflex generated by the bad experience of pain usually prevents further tampering with electricity. However, no matter how careful we are, accidents do happen and will continue to happen, especially among electrical workers, who must handle commercial electrical power lines every day.

Today, rates of electrical injury among industrial workers range widely from one country to another. Within industrializing countries, safety practices are often not the top priority, which results in higher rates of injury. In mature industrialized nations, electrical-shock rates continue to decline. In the United States, electrocution remains the fifth leading cause of fatal occupational injury, with an estimated economic impact of >$1 billion annually (1). Although accurate statistics are difficult to find, it appears that the rates of injury may be highest among electrical workers. A study in Virginia suggested that public utilities have the highest rate of fatal electrical injuries among all industrial sectors. One source indicates that, of these injuries, >90% occur in men, mostly between the ages of 20 and 34, who have 4–8 years of experience on the job (2). Another source (3) suggests that the average age of victims is 37.5 years, and the average experience amounts to 11.3 years. For survivors, the injury pattern is very complex, with a high disability rate caused by accompanying neurologic damages.

Away from the workplace, most injuries are caused either by indoor, low-voltage (<1000 V) household electrical contact or by outdoor lightning strikes (4). Low-voltage (120 V or 220 V), household power frequency electrical shocks are common and usually result in minor peripheral neurological symptoms or, occasionally, skin surface burns. However, more complex injuries may result, depending on the path taken by the current, particularly in small children after oral contact with household appliance cord disclosures or outlets (5). Compared with a high-voltage shock, which usually generates an arc and resulting explosive thermoacoustic blast, low-voltage shocks are more likely to produce a prolonged, "no-let-go" contact with the power source. This no-let-go phenomenon is caused by an involuntary, current-induced muscle spasm (6). For 60-Hz electrical current, the no-let-go threshold for axial current passage through the forearm is 16 mA for males and 11 mA for females (7, 8).

Injury often follows contact with higher-frequency electrical power as well. In the United States, ∼200 deaths are caused annually by lightning injury. Yet, many more people survive it. The range of extent for lightning injury is quite broad, depending on the magnitude of exposure and the condition of the victim. According

Annu. Rev. Biomed. Eng. 2000.2:477-509. Downloaded from arjournals.annualreviews.org
by UNIVERSITY OF CHICAGO LIBRARIES on 10/02/06. For personal use only.

to many reports, if lightning strikes in the vicinity of several individuals, usually only one endures serious or fatal injury. Radio frequency and microwave injuries are less common but nonetheless are important medical problems to understand. At higher frequencies, when wavelengths are short enough to couple at the atomic level, the fields can be ionizing and cause molecular heating.

In short, electrical trauma may produce a very complex pattern of injury, which is determined by multiple modes of frequency-dependent tissue-field interactions and variations in current density along the paths through the body, as well as variations in body size, body position, and use of protective gear. No two cases are the same. These variations create challenges in clinical diagnosis that often delay effective medical management. Further advancement in medical care of electrical shock victims will follow the development of more accurate bioengineering models of injury. Our objective is to review the basic considerations motivating additional bioengineering research.

Annu. Rev. Biomed. Eng. 2000.2:477-509. Downloaded from arjournals.annualreviews.org
by UNIVERSITY OF CHICAGO LIBRARIES on 10/02/06. For personal use only.

ELECTRICAL ENERGY TRANSPORT IN TISSUES

Broadly speaking, the human body is characteristically a segmented, nonuniform (or lumped-element), conducting dielectric. It consists of ~60% water by weight, in which 33% is intracellular and 27% extracellular (9). Body fluids in both the intracellular and extracellular compartments are highly electrolytic, and these two compartments are separated by a relatively impermeable, highly resistive plasma membrane. Current conduction within the body is carried by mobile ions in the body fluid. These mobile ions provide a conductivity of $\sim 1.4\ S\ m^{-1}$ in physiological saline. Because, in metal wires, the carriers for electrical current are electrons, the current carriers change from electrons to ions when in contact with the human body. This conversion occurs at the skin surface through electrochemical reactions (10).

At low frequencies (i.e. below microwave frequencies), current becomes distributed so that the electric field strength is nearly uniform throughout any plane that is perpendicular to the path of the current (11–13). As a consequence, the density distribution of electrical current depends on the relative electrical conductivity of various tissues and the frequency of the current. Experimental data support this basic concept. In 1981, Sances and coworkers measured the current distribution in the hind limb of anesthetized hogs (13). They found that the major arteries and nerves experienced the largest current density because of their higher conductivity. They also observed that skeletal muscles carried the majority of the current because of their predominant volumetric proportions.

At a more microscopic scale, low-frequency current distribution within tissue is determined by the density, orientation, shape, and size of cells. Because the cell membrane functions as an ionic-transport barrier, low-frequency electrical current is mostly shielded from cytoplasmic fluid. In addition, the presence of cells diminishes the area available for ionic current and, in effect, makes tissues less

TABLE 1 Electrical injury frequency regimes

Frequency regime	General applications	Harmful tissue effects
Low frequency (dc, 10 kHz)	Commercial electrical power, batteries	Joule heating, cell membrane electroporation
Radio frequency (10 kHz–100 MHz)	Radio-communication, diathermy, electrocautery	Joule heating, dielectric heating of proteins
Microwave (100 MHz–100 GHz)	Microwave heating	Dielectric heating of water
Light ($3.8–7.5 \times 10^{14}$ Hz)	Vision, laser applications	Molecular heating and photobleaching effects
Ionizing ($\geq 10^{15}$ Hz)	Ionizing irradiation (UV, X-ray, gamma, etc)	Atomic heating with generation of reactive oxygen intermediates

Annu. Rev. Biomed. Eng. 2000.2:477-509. Downloaded from arjournals.annualreviews.org
by UNIVERSITY OF CHICAGO LIBRARIES on 10/02/06. For personal use only.

conductive. As cell size increases, the membrane has less impact on a cell's electrical properties, because the volume fraction of the cell occupied by the membrane is proportionately decreased (14). Similarly, the resistivity of skeletal muscle that is measured parallel to the long axis of the muscle cells is less than that measured perpendicular to the axis. Solid-volume fraction is important too. For example, the resistivity of cortical bone and epidermis is higher than other tissues because their free-water content is lower.

The distribution of current through the body at higher frequencies, for example, in RF and microwave ranges, depends on other parameters. The cell membrane is no longer an effective barrier to passage of current, and capacitive coupling of power across the membrane readily permits passage of current into the cytoplasm. Factors affecting the field distribution in tissues include frequency-dependent energy absorption and the skin-depth. In the highest-frequency ranges, including light and shorter wavelengths, other effects such as scattering and quantum absorption become important in governing distribution of current through tissue. Table 1 categorizes the biological effects of electrical injury at various frequencies. Mechanisms of biological effects are different at each frequency level. A discussion of electrical-injury mechanisms must also be separated according to the frequency levels of the field.

PHYSICS OF TISSUE INJURY

Low-Frequency Electric Shocks

Until recently, a low-frequency electrical injury was considered only a thermal-burn injury, produced by Joule heating (6). Over the past 10 years, it has been shown that the pathophysiology of tissue electrical injury is more complex, involving thermal, electroporation, and electrochemical interactions (15–17) and blunt mechanical trauma secondary to thermoacoustic blasts from high-energy

TABLE 2 Modes of tissue injury in electrical trauma

Injury mechanism	Kinetics during electrical contact	Tissue susceptibility	Tissue damage distribution
Joule heating	1–10 s	All	All proteins, cell membrane
Electroporation	10^{-5}–10^{-4} s	Muscle, nerve	Membrane lipid bilayer
Electroconformational coupling in membrane proteins	10^{-3} s	Muscle, nerve	Membrane proteins
Thermoacoustic (blast)	10^{-2} s	All	Membrane structures

Annu. Rev. Biomed. Eng. 2000.2:477-509. Downloaded from arjournals.annualreviews.org
by UNIVERSITY OF CHICAGO LIBRARIES on 10/02/06. For personal use only.

arcs (18; Table 2). Although these forces can alter all tissue components, it is the thin plasma membrane of cells that is most vulnerable. Thus, the cell's plasma membrane appears to be the most important structure in determining the rate of tissue injury accumulation.

The most important function of the cell membrane is to provide a barrier against free ion diffusion. The energy required to move a solvated ion across a planar, pure-phospholipid bilayer in an aqueous, physiological environment approaches $\sim 68\, k_B T$ (19), indicating the steep energy hurdle. Because most metabolic energy of mammalian cells is ultimately invested in maintaining the ionic difference across the cell membrane (20), the importance of the structural integrity of the lipid bilayer is apparent. If the membrane is permeabilized, the work required to maintain transmembrane ionic concentration differences increases proportionately. The conductance of electropermeabilized membranes may increase by several orders of magnitude. ATP production and, in turn, ATP-fueled protein ionic pumps cannot keep pace, which leads to exhaustion of metabolic energy. If the membrane is not sealed, biochemical arrest will occur, and the permeabilized cell will become necrotic. Thus, in the present discussion of tissue injury resulting from electrical shock, the principal focus is on the kinetics of cell membrane injury and the reversibility of that process.

Direct Electric Field Effects A cell within an applied dc or low-frequency electric field will experience electric forces that act most forcefully across and along the surface of the cell membrane. The forces acting across the membrane can alter membrane protein conformation and disrupt the structural integrity of the lipid bilayer. The magnitude of the forces acting across the membrane is related to the induced transmembrane potential (V_m). V_m depends on a variety of factors, such as the intra- and extracellular conductivity of the medium, cell shape and size, and external electric field strength E, as well as how the electric field vector is oriented to the point of interest on the cell membrane (21–23).

Given that most cells are either spherical or cylindrical in shape, the expressions that describe the relationship between the externally applied electric field

Annu. Rev. Biomed. Eng. 2000.2:477-509. Downloaded from arjournals.annualreviews.org
by UNIVERSITY OF CHICAGO LIBRARIES on 10/02/06. For personal use only.

and V_m can be simplified to two forms. Considering physiologic conditions, the peak magnitude of V_m (V_m^p) at the electrode-facing poles of spherical cells can be expressed as

$$V_m^p = 1.5\, R_{cell} \cos(\phi) \cdot [1 + (f/f_s)^2]^{-1/2} \cdot E_{peak} \quad (1)$$

where R_{cell} is the radius of the cell, E_{peak} is the peak field strength in the tissue surrounding the cell, ϕ is the angle off axis from the field direction, f_s is the sub-β-dispersion frequency limit below which the cell charging time is short compared with rate of field change, and f is the field frequency. For cylindrically shaped cells, such as skeletal muscle and nerve cells, which are aligned in the direction of the field (herein assigned the z coordinate), V_m takes a different form. Under these circumstances an electrical space constant parameter becomes useful in describing the electrical properties of the cell. The V_m is expressed as

$$V_m^p(z) \approx A\, \lambda_m \sinh(z/\lambda_m) \cdot [1 + (f/f_s)^2]^{-1/2} \cdot E_{peak} \quad (2)$$

when λ_m is the electrical space constant of the cell, A is a variable that depends on cell length, and the position $z = 0$ corresponds to the midpoint of the cell. Figure 1 illustrates schematically the dependency of spatial variation of $V_m^p(z)$ on the cell size.

Equations 1 and 2 are valid as long as the electrical properties of the cell membrane remain constant. However, the major theme of this review is that the transport properties of the cell membrane are altered by forces that are much greater than the natural physiologic forces. The natural transmembrane potential of mammalian cells, which has a magnitude of <100 mV (24), originates from the difference in

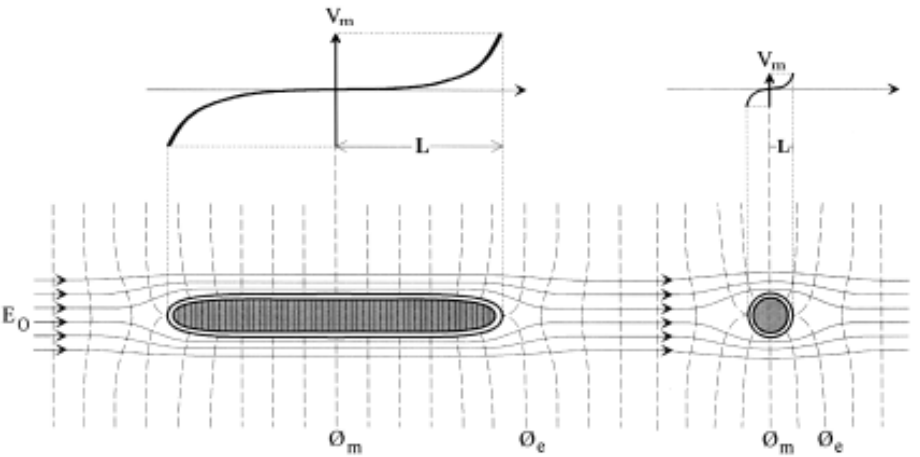

Figure 1 Dependence of cell size on the spatial variation of the induced transmembrane potential difference when cells are exposed to the same electric field. Electrical current lines are the same as electric field lines (E_0), and solid and constant voltage lines are *dashed*.

ionic strengths of the cell's intra- and extracellular fluids. When an imposed potential results in a transmembrane potential magnitude of >200 mV, intramembrane molecular alterations occur that may lead to membrane damage. The principal mechanisms of damage are electroporation of the lipid bilayer and electroconformational denaturation of the membrane proteins. Electroconformational damage to membrane proteins has been well documented for voltage-gated membrane protein channels. The processes occur quickly, on the order of milliseconds, after strong fields are applied.

Annu. Rev. Biomed. Eng. 2000.2:477-509. Downloaded from arjournals.annualreviews.org
by UNIVERSITY OF CHICAGO LIBRARIES on 10/02/06. For personal use only.

Electroporation. Electroporation is the term commonly used to describe the biophysical process of membrane permeabilization owing to electric field-driven reorganization of lipids in the lipid bilayer by supraphysiologic electrical fields (21, 25, 26). Contemporary electroporation theory indicates that highly electrically polar water molecules are pulled by Kelvin polarization stress into transient defects in the lipid packing order within a bilayer, leading to quasistable or stable pore formation. Although most commonly used to introduce foreign DNA into cells, electroporation has also been used on isolated cells to (*a*) introduce enzymes, antibodies, viruses, and other agents or particles for intracellular assays; (*b*) precipitate cell fusion; and (*c*) insert or embed macromolecules into the cell membrane. Recent reviews and books published have extensively treated this subject (21–23, 27–31). In this review we briefly examine this phenomenon as it relates to the understanding of electrical injury.

Electroporation can be either transient or stable, depending on the magnitude of the induced transmembrane potential, its duration, membrane composition, and temperature. The time required for electroporation ranges from 10s of microseconds to milliseconds. The physical state of the lipid bilayer, either liquid crystal or fluidic, is strongly temperature dependent. After application of a brief electroporating field pulse, the transiently electroporated membrane will spontaneously seal. Sealing follows the removal of water from the membrane defects. Sealing kinetics are often orders of magnitude slower than field relaxation because the forces driving the molecular sealing events are not as strong as the electroporating electric field. Sealing of electropores requires reordering of membrane lipids and removal of water molecules from the pore; both are time- and energy-consuming processes (32–34).

The threshold transmembrane potential for induction of membrane electroporation is remarkably similar across cell types. The threshold V_m for electroporation has been found to range from 300 to 350 mV (32–35). Several authors have developed models to explain the experimentally observed values of V_m that are required for electroporation and associated transmembrane aqueous dynamics (36, 37). With empirical data as parameters in an asymptotic approximation (38), the threshold V_m is predicted to be $\sim$250 mV, which is quite consistent with reported experimental data.

Generally, for most media-suspended, isolated cells with a typical diameter of 10–20 μm, the dc field strength threshold for electroporation is $\sim$1 kV cm^{-1}. By

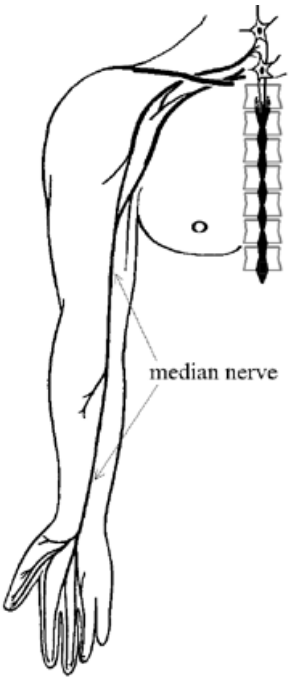

Figure 2 Anatomical sketch illustrating the length of nerve cells (e.g. median nerve), which makes them explicitly vulnerable to electric field-induced damage.

Annu. Rev. Biomed. Eng. 2000.2:477-509. Downloaded from arjournals.annualreviews.org
by UNIVERSITY OF CHICAGO LIBRARIES on 10/02/06. For personal use only.

comparison the fields required to alter large cells are much less. Owing to their relatively long lengths, skeletal muscle cells $\leq$8 cm long in large animals and nerve cells $\leq$2 m long have lower electroporation thresholds. Figure 2 illustrates the length scale of a large peripheral nerve such as the median nerve as an example. The peak transmembrane potential induced by an externally applied electric field scales with the dimensions of the cell in the direction of the applied field as shown in Figure 1. Therefore, muscle and nerve cell membranes are likely to be damaged with electrical fields as small as 60 V cm^{-1}.

The distribution of electropore formation in a cell placed in an applied field was recently addressed by DeBruin & Krassowska (39, 40). Expanding from previous theoretical models and including the fact that the membrane charging time of $\sim$1 μs is very short compared with a 1-ms field duration, they concluded that supraphysiological V_m at the pole caps is large enough to create pores and thereby effectively prevent a further increase in V_m in these areas.

This confirms early experimental findings, which show a saturation of V_m that is independent of the field strength (for high-voltage shocks, see 41–43). After the effect of ionic concentrations is included in the model, it is even possible to confirm asymmetries in V_m that are observed between the hyperpolarized (anode-facing) and hypopolarized (cathode-facing) poles of a cell (33, 34, 44). Although the pore sealing time (time needed for pores to close) in the range of seconds predicted by the model is in agreement with some published experimental results (45), others have

found longer sealing times, in the range of several minutes (32, 33, 46). This might be because (*a*) this model is based on pure lipid bilayers instead of cell membranes embedded with proteins and (*b*) it considers only primary pores formed by V_m (pores formed during shock) and not those formed after the external field pulse ends (secondary pores), the last of which provide transport routes for macromolecules.

Tissue Electroporation. Investigation of tissue electroporation was initially driven by the need for a better understanding of the pathophysiology of electrical injury (47, 48). In the early 1990s, tissue electroporation was studied in connection with cardiac defibrillation shocks (49, 50). More recently, it has begun to be envisioned as a potential therapeutic tool in the medical field. Tissue electroporation has found uses in (*a*) enhanced cancer tumor chemotherapy [electrochemotherapy (51, 52)], (*b*) localized gene therapy (53, 54), and (*c*) transdermal drug delivery and body fluid sampling (55–57). Computational models of human high-voltage electrical shock suggest that the induced tissue electric field strength in the extremities is high enough to electroporate skeletal muscle and peripheral nerve cell membranes (15, 58–60) and to possibly cause electroconformational denaturation of membrane proteins.

Bhatt and coworkers (15) measured electroporation damage accumulation in vitro in isolated, cooled rat *biceps femoris* muscles. After the initial impedance measurement, an electric-field pulse was delivered to the muscles with current pulses that set up tissue field pulse amplitudes ranging between 30 and 120 Vcm^{-1}, which was thought to be typical forearm field strengths in high-voltage electrical shock. The duration of the dc pulses ranged from 0.5 to 10 ms. These short pulses reduce Joule heating to insignificant levels. Field pulses were separated by 10 s to allow thermal relaxation. The change in the normalized low-frequency electrical impedance in the muscle tissue after the application of short-duration dc current pulses indicated skeletal muscle membrane damage. A decrease in muscle impedance magnitude occurred after dc electric field pulses that exceeded a 60-V cm^{-1} magnitude and a 1-ms duration. As seen in Figure 3, the field strength, pulse duration, and number of pulses were factors that determine the extent of electroporation damage.

Based on these results, Block et al (16) electrically shocked fully anesthetized female Sprague-Dawley rats through cuff-type electrodes wrapped around the base of the tail and one ankle (Figure 4), using a current-regulated dc power supply. The objective was to determine whether electroporation of skeletal muscle tissue in-situ could lead to substantial necrosis. The study involved histopathological analysis and diagnostic imaging of an anesthetized animal hind limb. A series of 4-ms dc pulses was applied, each pulse separated by 10 s to allow complete thermal relaxation back to baseline temperature before the next field pulse. The electric field strength produced in the thigh muscle was estimated to range from 37 to 150 V cm^{-1}, corresponding to applied currents ranging from 0.5 to 2 A. These tissue fields were suggested to be on the same levels as those experienced by many victims of high-voltage electrical shock. Muscle biopsies were obtained from the

Annu. Rev. Biomed. Eng. 2000.2:477-509. Downloaded from arjournals.annualreviews.org
by UNIVERSITY OF CHICAGO LIBRARIES on 10/02/06. For personal use only.

Annu. Rev. Biomed. Eng. 2000.2:477-509. Downloaded from arjournals.annualreviews.org
by UNIVERSITY OF CHICAGO LIBRARIES on 10/02/06. For personal use only.

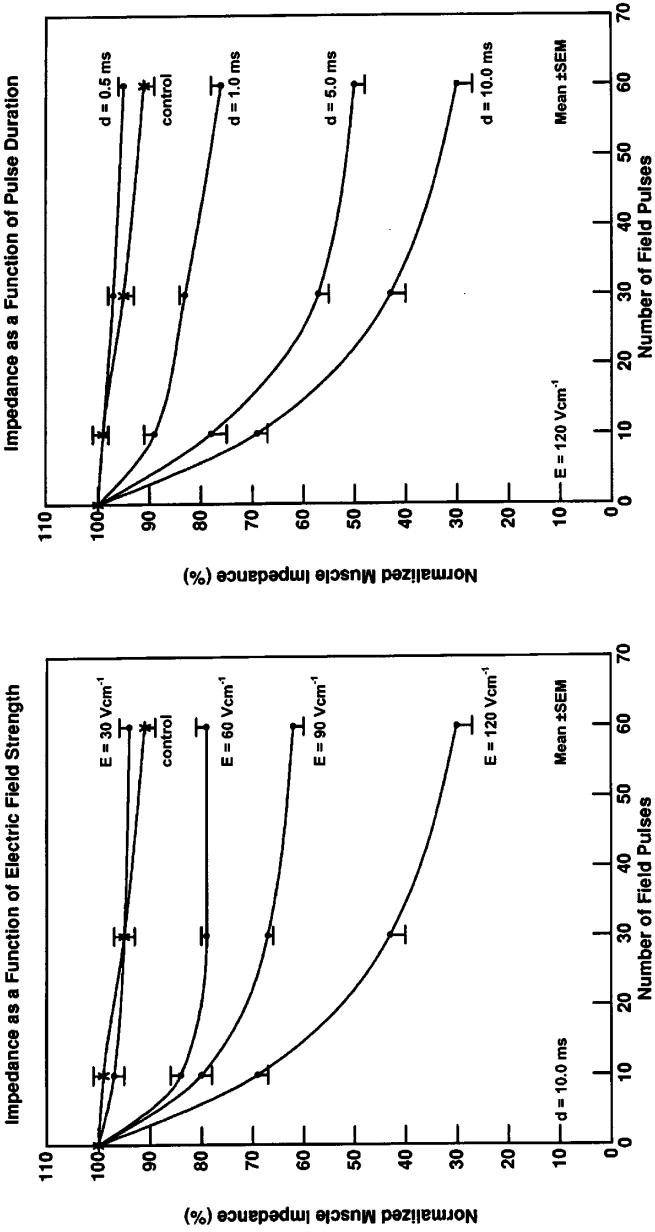

Figure 3 Muscle impedance magnitude plotted as a function of the number of electric field pulses delivered. *Left*: Each curve represents a different field strength E at a constant pulse width d of 10 ms. *Right*: the pulse width d is different for each curve, whereas E is held constant at 120 V cm^{-1} (mean $\pm$ SE, $N = 5$). The control (*) did not receive electric shock. (From reference 15, with permission.)

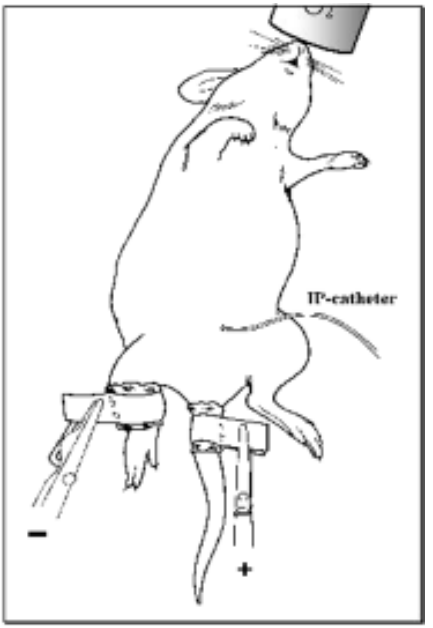

Figure 4 Electrode placement in the rat hind limb in vivo electrical-shock model.

Annu. Rev. Biomed. Eng. 2000.2:477-509. Downloaded from arjournals.annualreviews.org
by UNIVERSITY OF CHICAGO LIBRARIES on 10/02/06. For personal use only.

injured legs, as well as the collateral control legs, 6 h post-shock and subjected to histopathological analysis. Sections of electrically shocked muscle revealed extensive vacuolization and hypercontraction-induced degeneration band patterns, which were not found in nonshocked contralateral controls (Figure 5, see color insert). The fraction of hypercontracted muscle cells increased with the number of applied pulses. These results are consistent with the investigators' hypothesis that

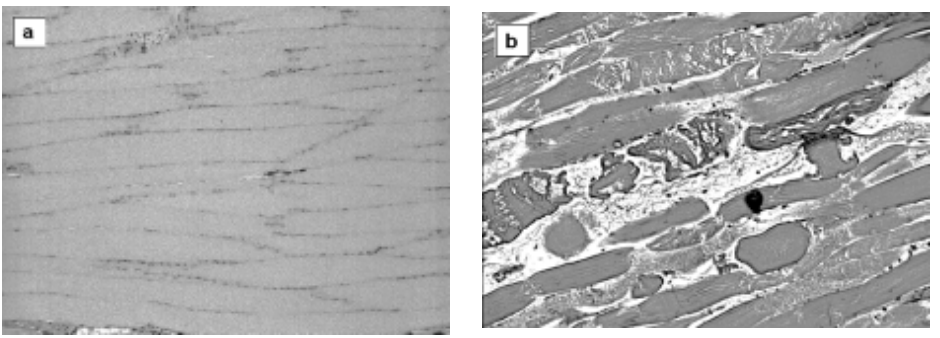

Figure 5 See color insert. Longitudinal histology sections of skeletal muscle tissue subjected to nine 4-ms dc-pulses with 2 A, 150 V cm^{-1} (*b*) compared with nonshocked control (*a*). Sections were stained with hematoxylin/eosin and show muscle cell damage in the form of extensive vacuolization and hypercontraction band degeneration; biopsy was taken at 6 h post-shock.

Annu. Rev. Biomed. Eng. 2000.2:477-509. Downloaded from arjournals.annualreviews.org
by UNIVERSITY OF CHICAGO LIBRARIES on 10/02/06. For personal use only.

nonthermal electrical effects alone can induce cellular necrosis. The pathologic appearance of the shocked muscle was similar to that seen in malignant hyperthermia, indicating that electroporation may lead to Ca^{2+} influx into the sarcoplasm. Most recently, a similar muscle injury pattern has been described by deBono in a clinical case report of a human electrical injury victim (61). These results suggested that direct electrical injury of skeletal muscle in situ can lead to the commonly seen pattern of injury in electrical shock victims, even in the absence of pathologically significant Joule heating.

Electrophysiological Responses to Electroporation. Records of compound muscle action potential (CMAP) amplitude reflect the vectorial sum of fields produced by individual action potential (AP) conducting muscle cells. Only cells with intact membranes and with active ATP production are capable of generating APs. Thus, changes in CMAP amplitude can be used to quantify the extent of tissue injury caused by events that damage cell membranes. In a recent report, CMAP recordings were used to estimate electroporation injury accumulation in the anesthetized rat hind limb. CMAPs were produced by magnetic stimulation of the distal spinal cord and were recorded via skin surface electrodes. With this entirely noninvasive protocol, CMAP changes in response to a series of applied 150-V cm^{-1} field pulses were recorded as a function of the number of field pulses applied. The data are shown in Figure 6. A saline injection was given intravenously 30 min after the electric field application to simulate fluid resuscitation and as a sham treatment for therapeutic investigations. The CMAP amplitudes decreased drastically after the electrical shocks were applied, and then they recovered gradually. The larger the number of shocks, the larger the initial drop in CMAP and the slower the recovery.

Imaging of Electroporation. ^{99m}Tc-pyrophosphate (PYP) is widely used as a radiolabel tracer for various forms of soft-tissue injury, including electrical trauma. It is known to accumulate in damaged soft tissue, to clear moderately quickly from undamaged tissue, and to deposit over time in bone. The biggest drawback in using ^{99m}Tc-PYP is that the mechanism of its accumulation in damaged tissue is not yet well understood; it is believed to follow the calcium movement in cellular function (62). Thus, increased tracer accumulation in the muscle tissue indicates loss of cell membrane integrity and tissue edema, and it is predictive of tissue damage.

Using the in vivo rat hind limb electrical injury model described by Block, Matthews (63) monitored the uptake of ^{99m}Tc-PYP in electrically shocked tissue as a function of the magnitude of the dc current. An application of 0.5, 1.0, or 1.85 A of dc was applied to the rat's hind limb. Intravenous saline infusion was used as sham treatment. For each animal, a series of ^{99m}Tc-PYP incorporation images (at 2-min intervals) over a period of 4 h was recorded. Matthews' results supported earlier reports indicating that ^{99m}Tc-PYP does accumulate in electroporated tissue. The plots of ^{99m}Tc-PYP incorporation in Figure 7 suggest that the level of tracer accumulation is positively correlated to the tissue field pulses applied. This

Annu. Rev. Biomed. Eng. 2000.2:477-509. Downloaded from arjournals.annualreviews.org
by UNIVERSITY OF CHICAGO LIBRARIES on 10/02/06. For personal use only.

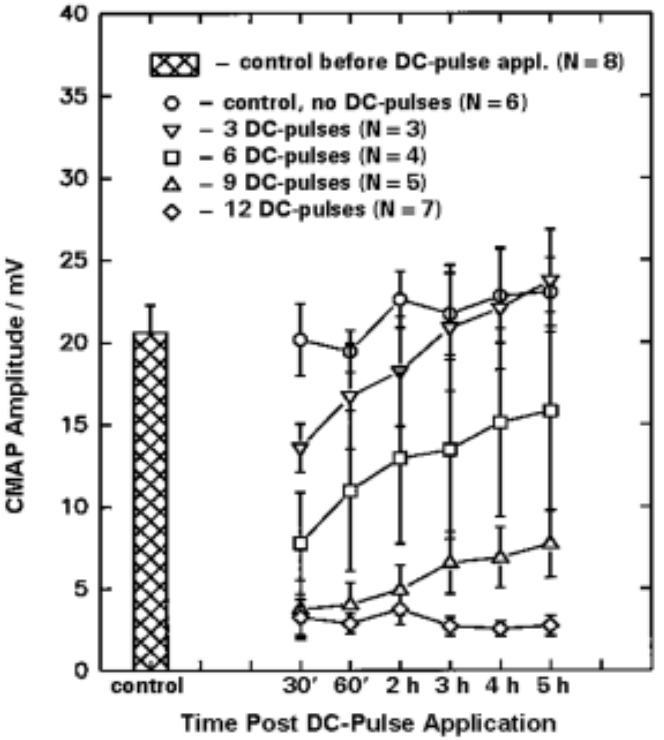

Figure 6 Changes in the compound muscle action potential (CMAP) in response to a series of 2-A dc pulses through the thigh (mean ± SE).

indicates that quantitative imaging of ^{99m}Tc-PYP uptake may be developed further as an indicator of the extent of electroporation or other membrane injury.

These experimental studies have shown that electroporation can lead to skeletal muscle tissue necrosis in vivo. The reasons that the accumulation dynamics of electroporation damage at the tissue level are different than for isolated cells include the reduction of membrane lipid mobility caused by adhesion to high-molecular-weight biopolymers in the extracellular matrix of tissues. In addition, the distribution of electric fields and, in turn, the V_m in tissue are influenced by the packing density of the cells. Collectively, these results suggest that electroporation is likely to be an important mechanism of injury in electrical-shock victims.

Thermal Burn Injury Passage of electrical current through Ohmic conduction leads to Joule heating that can cause severe burn injury in electrical-shock victims. "Burn injury" as used here specifically refers to tissue injury by damaging supraphysiological temperatures. Burn effects are related to protein alteration or denaturation, often followed by recognizable changes in the optical properties of

Annu. Rev. Biomed. Eng. 2000.2:477-509. Downloaded from arjournals.annualreviews.org
by UNIVERSITY OF CHICAGO LIBRARIES on 10/02/06. For personal use only.

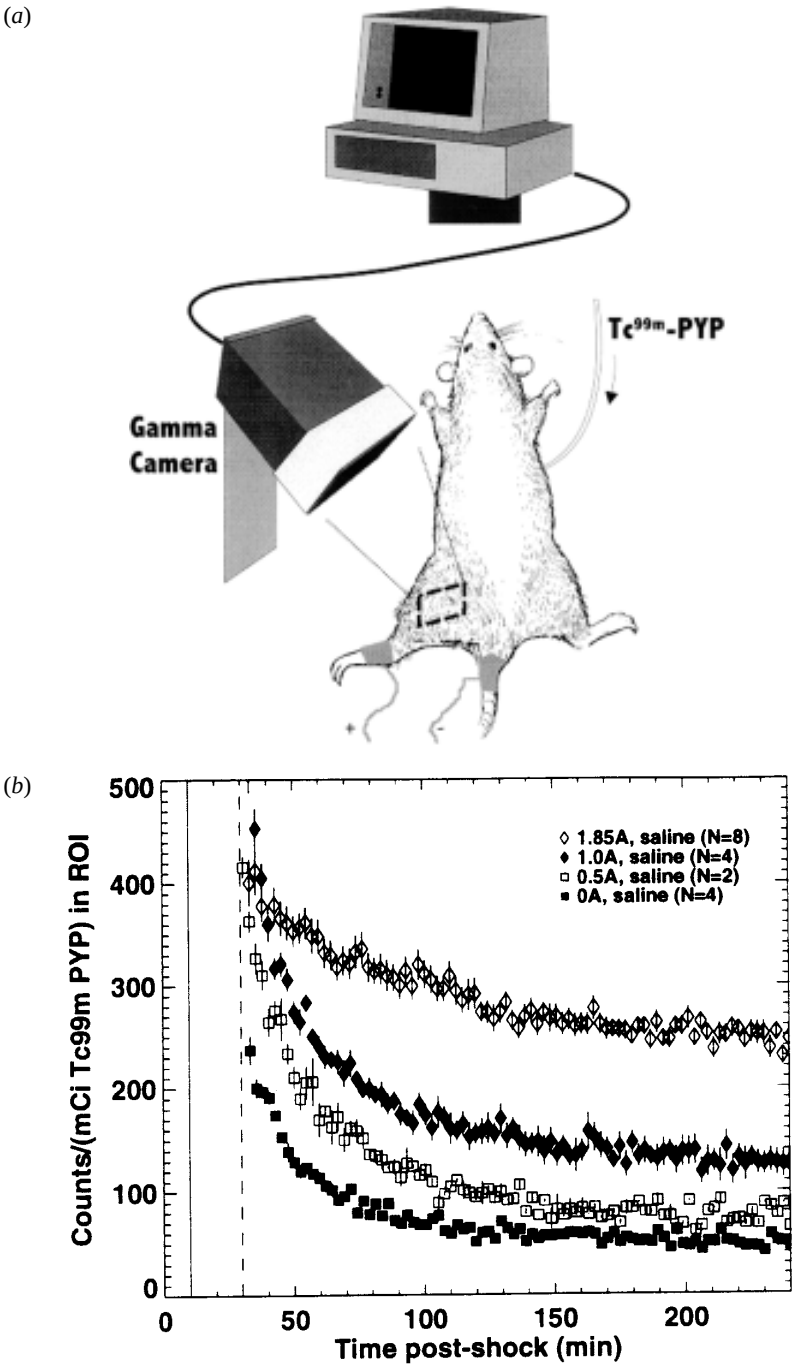

Figure 7 ^{99m}Tc-PYP time activity curves (TAC) after rat hind limb electrical shock (mean ± SE). Saline was injected 10 min post-shock (*solid line*); tracer was injected 30 minutes post-shock (*dashed line*) (From reference 63, with permission).

tissue. To understand the fundamental molecular basis of thermal burns, we must first recall that temperature, as defined by Boltzmann, is a measure of the kinetic energy of moving molecules of a medium. The relationship is defined by

$$k_B T \approx m v^2 \tag{3}$$

where k_B is Boltzmann's constant, v is the time-averaged speed of a monoatomic molecule in free solution at temperature T, and m is the mass of the molecule. As temperature rises, both the frequency of intermolecular collisions and the molecular momentum transfer between colliding molecules increase. When sufficient energy is transmitted to a macromolecule, an alteration in its molecular conformation can take place. As a consequence, at supraphysiologic temperatures, the probability that macromolecules such as proteins will depart from their native structures increases.

There are two conceptually different potential outcomes for the denatured protein, which depend on the initial molecular structure and configuration. The first possibility occurs when the native folded conformational state of the protein, held by intramolecular bonds, is different from the most favored conformation when no intramolecular cross-links are needed to maintain the native folded state (the thermodynamically lowest energy level). When such a protein is heated, the intramolecular bonds are broken, and it is denatured to one of several preferred lower-energy states from which it will not spontaneously return to the native conformation. Conceivably, if the primary structure of the protein is undamaged, it may be plausible to reconfigure the protein by using similar chaperone-assisted mechanisms that established its initial folding after biosynthesis. The second possibility occurs when the native folded state of the protein is the same as the most preferred, lowest-energy protein conformation in the absence of intramolecular cross-links. Because the preferred configuration of a non–cross-linked protein is temperature dependent, proteins will become heat denatured into conformations that are different from the preferred conformations at normal operating temperatures. The free-energy, G, and hence the relative stability of any state of a protein is governed by competing tendencies—the tendency to form as many bonds as possible, measured in units of enthalpy, H, and the tendency to be as disordered as possible, measured in units of entropy, S. Because S is scaled by temperature, it has to be multiplied by temperature to get the energy. Thus, $G = H - TS$.

When the temperature is raised to a higher level, the thermodynamic energy profile changes; the denatured form then has the lower energy, and the activation energy barrier between different conformations is much lower. It is then energetically possible and favorable for the protein to be denatured. When the temperature is lowered to the normal body temperature, the landscape changes again, effectively trapping the protein in the damaged state owing to the again higher activation barriers.

The speed of the transition from natural to denatured states is governed by the Arrhenius rate equation, which states that, when the kinetic energy of the molecule exceeds a threshold magnitude E_a^i (for activation energy), the transition to the ith

Annu. Rev. Biomed. Eng. 2000.2:477-509. Downloaded from arjournals.annualreviews.org
by UNIVERSITY OF CHICAGO LIBRARIES on 10/02/06. For personal use only.

state will occur (in this case from natural to denatured state). For a large number of molecules at temperature T, the fraction with a kinetic energy above E_a is governed by the Maxwell-Boltzmann relation (Γ) (64),

$$\Gamma^i = \exp\left(-E_a^i / k_B T\right) \tag{4}$$

where k_B is Boltzmann's constant. Because the strength of bonds retaining the folding conformation of macromolecules is very dependent on the nature of the chemical bond, the value of E_a^i is dependent on molecular structure. Despite this complexity, the net rate of denaturation of cellular structures containing many different proteins is also often describable in terms of Equation 4. For example, the accuracy of this equation in describing thermal damage to cell membranes has been reported (65–67). Even the thermal injury to intact tissues like human skin is reasonably described by this simple equation. It has been known for >50 years that the rate at which damage accumulates in heated skin can be estimated by convolving Equation 4 with the temperature history. The resulting expression is called the "heat damage" equation (68),

$$\mathrm{d}\Omega/\mathrm{d}t = A\Gamma \tag{5}$$

where Ω_B is a parameter that is reflective of the extent of damage and A is a frequency factor that describes how often a change in configuration actually occurs when such a reaction is energetically possible, which is also very dependent on molecular structure. The shape of the temperature-time curve predicted by Equation 5 is indeed the same as the human skin temperature-vs-time scald burn curve measured by Henriques & Moritz (69). This temperature-time curve shape has also been obtained for heat damage to isolated cells (67).

Because the lipid bilayer components of the cell membranes are held together only by forces of hydration, the lipid bilayer is the most vulnerable to heat damage (70). Even at temperatures of only 6°C above normal (i.e. 43°C), the structural integrity of the lipid bilayer is lost (71). In effect, the warmed lipid bilayer goes into solution, rendering the membrane freely permeable to small ions. Published reports indicate that the contractile mechanism of muscle cells is destroyed at slightly higher temperatures, immediately after exposure to temperatures of 45°C and above (72). Experiments on fibroblasts have demonstrated that heat-induced membrane permeabilization also begins to appear at temperatures of >45°C (73).

Bischof and coworkers investigated the effect of supraphysiological temperatures on isolated rat muscle cells by using a thermally controlled microperfusion stage (74). Cells were loaded with the membrane-permeable fluorescent dye precursor calcein-AM. After entering the cell, the precursor is converted by nonspecific esterases into membrane-impermeable fluorescent calcein. By quantitative fluorescent microscopy, Bischof et al measured time-resolved dye leakage from the muscle cells at several supraphysiological temperatures (Figure 8). In addition, using Equations 4 and 5, the authors determined the activation energy necessary to thermally induce membrane permeabilization in the isolated muscle cells to be

Annu. Rev. Biomed. Eng. 2000.2:477-509. Downloaded from arjournals.annualreviews.org
by UNIVERSITY OF CHICAGO LIBRARIES on 10/02/06. For personal use only.

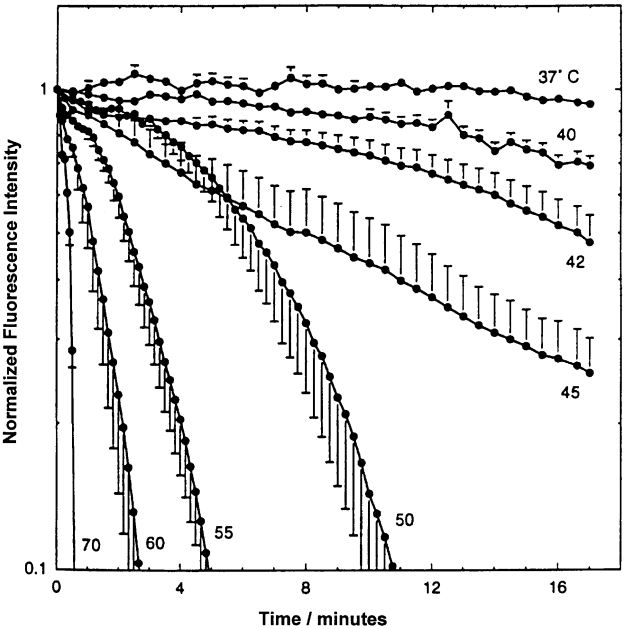

Figure 8 Intracellular calcium content vs time at specified temperature. The optical stage is designed to allow rapid heat clamp readings (From reference 74, with permission).

Annu. Rev. Biomed. Eng. 2000.2:477-509. Downloaded from arjournals.annualreviews.org
by UNIVERSITY OF CHICAGO LIBRARIES on 10/02/06. For personal use only.

32.9 kcal mol^{-1} (74). Reported activation energy values for thermal damage in other cell types are in the range from 30 to 140 kcal mol^{-1} (67).

Electroconformational Denaturation of Transmembrane Proteins In addition to membrane electroporation, which is mainly a lipid bilayer phenomenon, large supraphysiologic V_m can produce electroconformational changes of membrane proteins, ion channels and ion pumps. Of a cell's membrane, ~30% consists of proteins, some of them embedded into the bilayer and others spanning the entire membrane. Many of these proteins carry electric charges from amino acids with acidic or basic side groups that can be acted on directly by an intense V_m (charge separation or charge induction through dissociation). In addition, each amino acid has an electrical dipole moment of ~3.5 D (Debye $= 3.336 \cdot 10^{-30}$ Cm), giving the proteins an overall dipole moment that, for an α-helical protein structure, can reach 120 D (75). In a strong external electric field, those molecules will orient themselves and thereby change their conformation to increase the effective dipole moment in the direction of that field.

If the field strength becomes sufficiently intense, those field-induced changes can cause irreversible damage to a membrane protein. In particular ion channels and pumps, with their selective, voltage-gated charge transport mechanisms (e.g. Ca^{2+}-specific channel), are highly sensitive to differences in V_m. Chen and coworkers

(76, 77) investigated the effects of large-magnitude V_m pulses on voltage-gated Na^+ and K^+ channel behavior in frog skeletal muscle membrane, with a modified double petroleum jelly-gap voltage clamp. They found, in both channel types but more drastically in K^+ channels, reductions of channel conductance and ionic selectivity by the imposed V_m (76). In their most recent work, Chen et al were able to demonstrate that these changes are not caused by the field-induced huge channel currents (Joule heating damage) but rather the magnitude and polarity of the induced V_m (77). The consequences of this effect may underlie the transient nerve and muscle paralysis in electrical injury victims.

Annu. Rev. Biomed. Eng. 2000.2:477-509. Downloaded from arjournals.annualreviews.org
by UNIVERSITY OF CHICAGO LIBRARIES on 10/02/06. For personal use only.

RF and Microwave Burns

Although relatively less common, each year many cases of RF or microwave field injuries occur. Above the low-frequency regime (>10 kHz), tissue response strongly depends on the field frequency. In the 0.1- to 100-MHz RF range, two types of tissue heating occur, Joule and dielectric heating, with Joule heating outweighing dielectric heating. Small molecules like water, when not bound, are able to follow the field up to the gigahertz range (78). However, at microwave frequencies (100 MHz–100 GHz), dielectric heating is more significant than Joule heating because both bound and free water are excited by microwaves. A water molecule has a small size but a large dipole moment; hence, water has a strong perceptivity to microwaves, which induces water molecules into rapid oscillative rotation and in turn heats up the whole tissue. If the amplitude of the field strength is constant, the heating rate increases with field frequency until the viscous drag on the rotating molecule makes it lose pace with the field. Molecular dipoles of larger sizes oscillate more slowly, so that their most efficient induction frequency is in the RF range. For example, coupling of RF energy into proteins and DNA molecules is the basis of recent concerns about cellular phones. The therapeutic use of RF hyperthermia is based on the same mechanism.

Exposure to ambient microwave fields is known to cause burn trauma. Microwave burns have different clinical manifestations than low-frequency electrical shocks (79–82). At low frequency, the epidermis is a highly resistive barrier, whereas in the microwave regime, electrical power readily passes the epidermis in the form of capacitive coupling, with very little energy dissipation. Consequently, the epidermis may not be burned unless it is very moist. The microwave field penetration into tissue has a characteristic depth in the range of 1 cm, resulting in direct heating of subepidermal tissue water. The rate of tissue heating is dependent not only on the amplitude of the tissue electric field, but also on the density of dipoles. For example, microwave heating is much slower in fatty tissues (83).

Lightning Injury

Lightning arcs result from dielectric breakdown in air caused by build up of free electrical charges on the surface of clouds. The current through an arc can be

enormous, but the duration is quite brief (1–10 ms). The primary current is confined to the surface of conducting objects connected by the arc. Peak lightning current ranges between 30,000 and 50,000 A, which can generate temperatures near 30,000 K. This abrupt heating generates a high-pressure thermoacoustic blast wave known as thunder.

An individual directly struck by lightning will experience current for a brief period of time. Initially, the surface of the body is charged by the high electric field in the air. This can cause breakdown of the epidermis and several hundred amperes to flow through the body for a 1- to 10-μs period, which is certainly long enough to induce electroporation. After this, a much smaller current persists for several milliseconds, in which time the body is discharging into the ground. The duration of current flow is relatively short, so there is no substantial heating except a breakdown of the epidermis. However, disruption of cell membrane can wreak havoc on nerve and muscle tissues.

When lightning reaches the ground, it spreads out radially from the contact point. A person walking nearby can experience a substantial shock current, if the feet are widely separated. For example, with an average lightning current of 20,000 A, a step length of 50 cm, and an individual located 10 m away from strike point, the voltage drops between the legs can reach 1500 V. This can induce a 2- to 3-A current flow through the body between the legs for a 10-μs period.

The immense current pulses in lightning induce large magnetic-field pulses in its surrounding. The magnetic-field pulses set up secondary electrical currents inside any charge carrying matter inclusive living organisms. The secondary currents, forming closed loops around the penetrating magnetic-field lines, are, in theory, large enough to cause cardiac arrest, seizures, and other harmful effects. Also, electrical currents are induced through any electrical circuits penetrated by the magnetic field. Consider the scenario of a person standing on wet ground and leaning on a metal golf club. The golf club links the upper body to the soil, which, in effect, forms a closed loop consisting of golf club, body and wet soil. A large magnetic pulse can drive large currents through this circuit.

Ionizing Radiation

Radiation injury occurs after exposure to damaging levels of an ionizing particle beam or of electromagnetic irradiation, both of which alter the atomic structure and lead to damaging chemical reactions. Radiation injuries are often called burns although heating is totally insignificant. The most common radiation injury happens after excessive UV light exposure, often referred to as sunburn.

Mechanistically, electromagnetic waves of frequencies greater than UV light can excite electrons in an atom, leading to the formation of unpaired electrons in the outer electron orbital. In biological tissues, this results in damage to proteins, polysaccharides, and lipids (84). The reactive species from photoionization of water are primarily reactive hydroxyl radicals that can attack biological macromolecules, leading to altered chemical bonding, altered molecular structure, and,

Annu. Rev. Biomed. Eng. 2000.2:477-509. Downloaded from arjournals.annualreviews.org
by UNIVERSITY OF CHICAGO LIBRARIES on 10/02/06. For personal use only.

ultimately, blocked biological functioning of these macromolecules. The hydrogen bonds in DNA and proteins are particularly vulnerable. This vulnerability is the rationale behind the use of radiation in cancer therapy and its use in other procedures to block cell proliferation (85).

Because some free radicals have no net electrical charge, they have relatively free access to the lipid bilayer (86). Although the precise molecular mechanisms of membrane permeabilization are still under investigation, some researchers suggest that it is mainly caused by membrane lipid peroxidation; protons get stripped off from their carbon backbone in the membrane lipids, leading to desaturation in their structure (86). Polyunsaturated fatty acids are bulkier and tend to self-aggregate by lateral diffusion in the lipid bilayer, which leads to bilayer instability and poration (87).

Clinical manifestations begin when the rate of free-radical generation exceeds the cell's ability to scavenge free radicals. DNA is particularly susceptible to free-radical–mediated, abnormal cross-linking. This process forms the basis for cancer radiotherapy, in which a carefully calibrated dose of radiation is delivered to a tumor to damage only its DNA, with tolerable adverse effects on other macromolecules. If the dosage is too high compared with the patient's scavenging ability for free radicals, tissue injury occurs. As a consequence, visible tissue changes appear as cell injury triggers the tissue inflammation cascade. This radiation-induced inflammation, particularly that caused by sunburn, is very similar in appearance to that produced by superficial thermal burns.

Annu. Rev. Biomed. Eng. 2000.2:477-509. Downloaded from arjournals.annualreviews.org
by UNIVERSITY OF CHICAGO LIBRARIES on 10/02/06. For personal use only.

ANATOMIC PATTERNS OF INJURY

The location and extent of tissue damage depend on the field strength, frequency, duration of contact, and tissue properties. The pattern of injury in a shock victim also depends on the path of the current through the body, the protection provided by clothing, the victim's health status, the presence of a thermoacoustic blast, and fractures caused by muscle spasm, seizures, etc. The type and pattern of injury are of central importance to the clinical management of the victim.

Commercial-Power Frequency Injuries

Estimating Thermal-Injury Patterns The first task in understanding clinical patterns of electrical injury is to estimate the tissue field strength along the path taken by the current. A computer model, first reported by Tropea & Lee, was used to estimate the field distribution in a sample human upper extremity (58). Because of variations in anatomic contact, use of protective equipment, and power source parameters, they assumed a simplified worst-case scenario of perfect mechanical and electrical contact. The worst case was considered to be a perfect mechanical contact with bare, wet hands and a hand-to-hand current path. They numerically solved Laplace equations for the electric field in human upper limbs using a fully

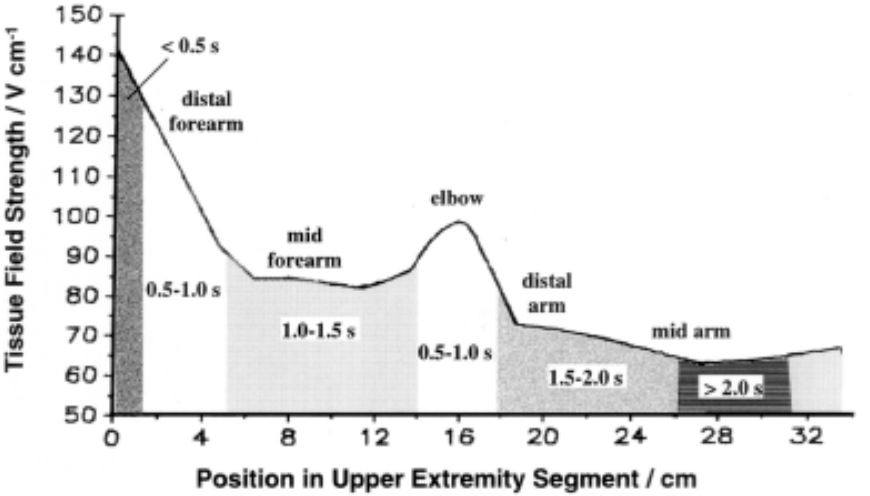

Figure 9 Magnitude of the axial electric field distribution across the chosen arm segment during 10-kV hand-to-hand contact. The field varies by the cross-sectional area and the cross-section's tissue composition (see text). The shaded areas indicate the contact time required for the tissue temperature to reach 45°C in the respective areas.

three-dimensional, finite-element computational model based on an average male adult body, including average size and shape and the position of skin, fat, muscle, and bone as indicated by a standard anatomical cross-sectional atlas (88). From this, the Joule heating dynamics in tissues during and after high-voltage electrical shock were derived (58). These simulations were based on a hand-to-hand potential drop ranging from 1 to 20 kV. The resistance for a single upper extremity was calculated to be 384 ohm, and the total hand-to-hand resistance was 1268 ohm, which agreed well with Freiberger's measurements (89) made more than 60 years ago. The calculated electric field strength in the upper extremity for a worst-case contact with a 10-kV hand-to-hand, 60-Hz source was found to be highest in the distal forearm owing to its small cross-section, where the field ranged from 65 to 140 V/cm (Figure 9). The field strength attains maxima at the joints reflecting the high percentages of bone and skin in the anatomic cross-sections at these locations. Appropriate thermal and electrical properties were assigned to each tissue, and the temperature rise caused by Joule heating was determined with the Pennes bioheat equation (90), with an added energy source term for Joule heating. This equation describes the balance between heat dissipation caused by conduction heat transfer and cooling through blood perfusion and heat generation caused by electric current. The result was the temperature profile for each anatomic cross-section as a function of duration of current flow (i.e. contact) and the contact voltage. Tropea & Lee (58) found that, when the tissues were electrically connected in parallel, skeletal muscle sustained the largest temperature rise and then heated adjacent tissue.

Annu. Rev. Biomed. Eng. 2000.2:477-509. Downloaded from arjournals.annualreviews.org
by UNIVERSITY OF CHICAGO LIBRARIES on 10/02/06. For personal use only.

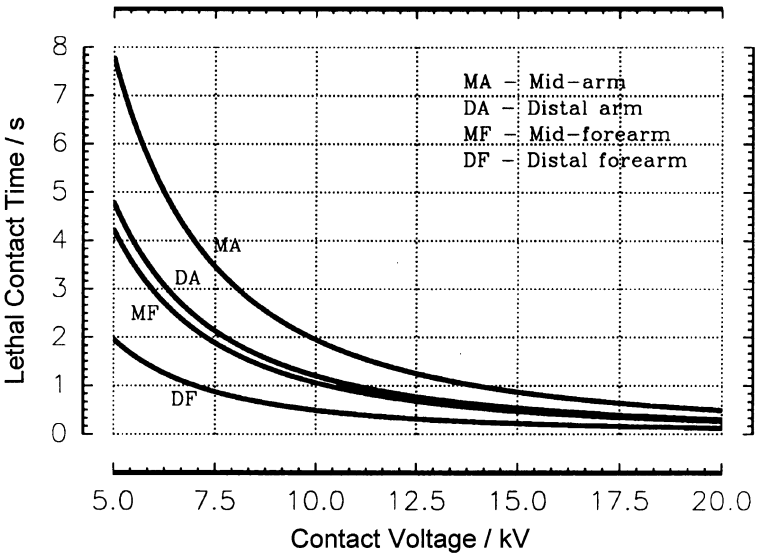

Figure 10 Lethal contact time for points selected in the center of the muscle mass for various cross-sections of the arm, computed for a 10-kV hand-to-hand contact. (From reference 58, with permission.)

Annu. Rev. Biomed. Eng. 2000.2:477-509. Downloaded from arjournals.annualreviews.org
by UNIVERSITY OF CHICAGO LIBRARIES on 10/02/06. For personal use only.

In addition, the tissue perfusion was found to be the most important parameter in determining the kinetics of tissue cooling. Estimates of lethal contact times (LTs) required to produce substantial heat damage at any point in the model were derived by convolving Equation 4 with the tissue temperature history for a number of adjacent points in the center of muscle in selected anatomic cross-sections. The LTs were defined by solving for the time for $\Omega = 1$ in Equation 5. The LTs were determined for points selected in the center of the muscle mass for various cross-sections as shown in Figure 10. The four curves displayed represent the LTs of contact as a function of contact voltage at different positions along the axis of the upper extremity. These values would be different if the size of the upper extremity changed, if the shape changed as would occur in a change in position, if the electrical contact was mediated by an arc, or if other deterministic parameters changed.

The LT curves are helpful to estimate the likelihood of significant thermal damage after an electrical-shock exposure. Unfortunately, the contact time of an actual electrical shock injury is almost never known. It seems, from the work of Jones et al (91), that for accidents involving high-power electrical sources, contact times are very likely to be only fractions of a second, because the acoustic blast resulting from arcing is likely to push the victim away, whereas longer contacts are more likely with lower voltages. Thus, the usefulness of the LT analysis rests in its suggestion that the duration of contact is the most significant parameter in

determining the extent of thermal injury to subcutaneous tissues in high-voltage, high-current electrical shock.

Imaging Electroporation Damage Patterns In most electrical-injury cases, the treating physician does not know the voltage, current, and contact time experienced in a particular high-voltage accident. Because the muscle damage sustained lies invisible underneath the skin, noninvasive-imaging methods such as magnetic resonance imaging (MRI) have been explored as important tools in early diagnosis. Proton-MRI allows the detection of the edema (T_2-weighted imaging sequences) and evaluation of permeability changes (contrast enhanced T_1-weighted sequences) in electrically induced muscle injury with high spatial resolution.

Using the previously described rat hind limb electrical-injury model, Hannig et al acquired multislice T_2-weighted and contrast agent Gd-DTPA (gadolinium-diethylenetriaminopenta acetic acid)-enhanced T_1-weighted images to obtain information about edema localization and contrast agent distribution volume, respectively (92). Images of relative distribution volume of contrast agent distribution in the electrically shocked hind limb were obtained by subtracting the preinjection T_1-weighted image sets from the respective postbolus-injection T_1-weighted image sets (93). MRI scans of nonshocked rat hind limbs served as a control for image interpretation. Significant differences in both the T_2- and contrast-enhanced T_1-weighted images were observed between control (nonshocked) and electrically shocked animals (Figure 11). The investigators found a strong regional correlation between edematous tissue (T_2) and areas of increased contrast agent distribution volume (T_1), confirming the cell membrane-permeabilizing (electroporating) nature of the muscle injury that was imaged.

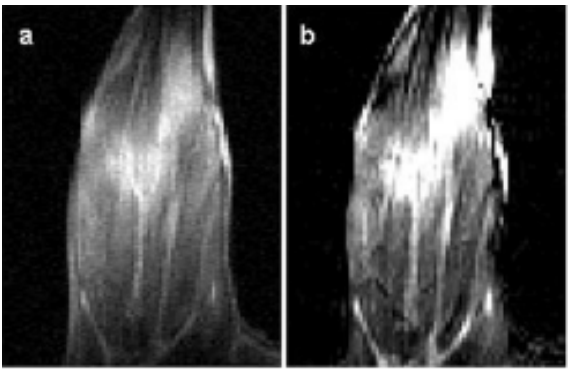

Figure 11 Magnetic resonance images of electrically shocked rat hind limb (9 pulses, 2 A, 150 V cm^{-1}, 4-ms duration, 10-s interval). Edematous areas are shown by T_2-weighted image (*a*) and regionally correlate well with areas of increased distribution volume, shown in the contrast enhanced (Gd-DTPA) T_1-weighted difference image [*b* (identical slice)].

Annu. Rev. Biomed. Eng. 2000.2:477-509. Downloaded from arjournals.annualreviews.org
by UNIVERSITY OF CHICAGO LIBRARIES on 10/02/06. For personal use only.

Annu. Rev. Biomed. Eng. 2000.2:477-509. Downloaded from arjournals.annualreviews.org
by UNIVERSITY OF CHICAGO LIBRARIES on 10/02/06. For personal use only.

Because muscle bundles are encapsulated in layers of perimysium and epimysium, severe edema will increase the local interstitial hydrostatic pressure so much that it obstructs the local blood flow (compartment syndrome). The prolonged ischemia alone will also cause muscle necrosis. This effect is especially pronounced in deep muscles that are injured by electric shock (5). As discussed by Lee (5), if edema is present in a muscle group, damage should be expected. The MRI images of electrically shocked hind limbs shown in Figure 11 demonstrate also that electrical injury is not uniformly distributed in the bulk muscle tissue; some muscle flaps are spared, and others endure more severe damage. The inhomogeneous injury pattern of muscle electrical injury is probably a combination of the following factors: (*a*) nonuniform distribution of electrical-current intensity in different muscle flaps; (*b*) nonuniform electrical resistance distribution of muscle itself and the break-in barrier resistance of muscle sheaths; (*c*) differences in relative orientation of different muscle cell bundles and muscle flaps with respect to the electrical-current entrance and exit points. Although at this time we can only speculate on the cause for the inhomogeneous injury pattern, the early differentiation of injured vs noninjured muscle flaps via MRI will greatly help treating physicians in surgery planning and management.

Combined Thermal- and Electrical-Injury Mechanisms The preceding discussion indicates that there are thermal and direct electrical mechanisms of tissue injury in victims of electrical shock. These mechanisms produce different cellular injuries, suggesting that therapeutic strategies should be different. Thus it is important to discuss this important matter further.

Because of the universal vulnerability of all tissue types to supraphysiologic temperature exposure, prolonged contact causes direct thermal damage to all tissues in the current path. For tissue field strengths of >30 V cm^{-1}, generation of heat is so much faster than the heat convection from blood perfusion that the heating process is considered quasiadiabatic. Clearly, as boiling and vaporization begin (which dissipate heat much more quickly), this approximation no longer holds.

Significant membrane permeabilization in human skeletal muscle cells with average lengths can occur in field applications of >25 V cm^{-1} for any contact time of >20–40 ms. However, the extent of the Joule heating-mediated damage depends on the duration of the contact. Figure 12 shows that, if the field strength is <25 V cm^{-1}, it will never heat up a tissue with normal blood circulation. On the other hand, all field exposure levels shown lead to membrane permeabilization. At higher field strengths, the combination of field strength and exposure time to reach certain tissue temperatures is plotted as separate curves. At higher field strengths, a lower exposure time is needed to reach the same temperature by way of Joule heating.

The importance of the duration of contact is again illustrated in Figure 9. For a fixed-current (10-A) contact, the electric-field strength in the tissue as a function of the position along the arm is plotted as derived from the three-dimensional model described above. The shading underneath the curve reflects the variation

Annu. Rev. Biomed. Eng. 2000.2:477-509. Downloaded from arjournals.annualreviews.org
by UNIVERSITY OF CHICAGO LIBRARIES on 10/02/06. For personal use only.

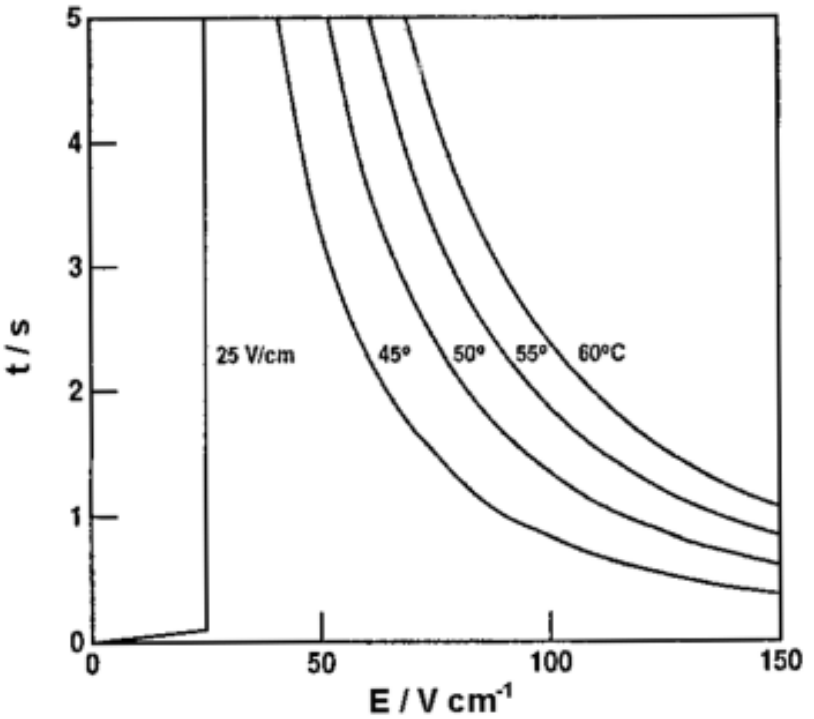

Figure 12 Electric field strength and contact duration required for cellular damage by thermal and electrical mechanisms. Membrane permeabilization occurs at fields >25 V cm^{-1} and for any contact time longer than 20–40 ms. For large fields or long contact duration, electrically induced membrane structural breakdown is masked by thermally induced damage, as shown by the temperature curves.

in predicted contact time as a function of position needed to raise skeletal muscle tissue temperature from 37°C to 45°C. As mentioned earlier, heat-induced cellular membrane damage accrues in a temperature-dependent fashion >42.5°C (67, 74). Obviously the tissue sections experiencing higher field strengths require less exposure time to produce a temperature rise to 45°C and above.

The predicted combined electroporation and thermal-injury distribution after electric shock, as suggested in Figure 9 in the human upper-extremity model, provides some insight into the variation in injury pattern when contact duration and strength are known. Clearly, brief-duration contacts, on one hand, result in membrane breakdown without significant burn injury. High-field or long-duration contacts, on the other hand, usually result in thermal damage and may overshadow the effect of electroporation on clinical outcome. Additional simulations of this nature with morphable models would be useful for further insight. Simulations that include the changes in tissue properties as a function of applied field strength,

hydration state, and temperature (which changes its chemical nature) would also be quite important. In a recent report by DeBono (61), a 100-kV–injured human arm (with the current path running from palm to shoulder) was amputated and dissected. He found that, on the forearm, the damage (to both the muscle and the nerve tissue) was much more severe on the radial (thumb) side than on the ulnar side, which would not be predicted by assuming constant and uniform tissue properties.

Even if the bulk tissue has a uniform field strength, different muscle cells will be injured differently, owing to differences in cell size, orientation, and anatomical site, as demonstrated by the theoretical model of Gaylor et al (14). For example, a long muscle aligned in parallel with the field gradient will experience a much larger transmembrane potential than one aligned perpendicular to it. Gaylor et al suggested that, under certain assumptions, skeletal muscle cells in the interior of a bundle may experience a higher level of V_m than those near the exterior fascia, and cells next to a bone will experience a higher V_m than those away from it. These predictions seem to agree with the general injury pattern reported (94–96) as well as experimental observations (92).

Annu. Rev. Biomed. Eng. 2000.2:477-509. Downloaded from arjournals.annualreviews.org
by UNIVERSITY OF CHICAGO LIBRARIES on 10/02/06. For personal use only.

Microwave and Radio Frequency Burns

Of a few reports on microwave injuries in the literature, a large portion of these injuries result from use of RF electrocautery devices during surgery, in which microwaves are used to heat denature proteins, thereby controlling bleeding, or to rapidly vaporize tissue water before cutting (97). Use of these devices will occasionally result in unintentional tissue injury. Most of the injury occurs below the epidermis, with the fat tissue largely spared. Fat does not attenuate the field well either. Skeletal muscle has a high level of hydration; hence it carries a heavy load of thermal input when subjected to microwaves. Clinical experience indicates that a characteristic "layered burn" occurs, consisting of burned skin and muscle with fat spared in between.

Microwave burns demonstrate similar patterns to those from the higher-frequency RF burns. However, there is more of a Joule heating component in RF heating; hence fat is not as well spared as in microwave heating. Another more common complication of RF hyperthermia procedures is nerve injuries (78). Therapeutic guidelines on RF hyperthermia require that tissue temperature be maintained at 42°C–43°C. Exposure to this temperature for 0.5–1 h will generate substantial heat-mediated membrane permeabilization. Patients with RF burns usually have deep fourth-degree burns that penetrate all tissues. Most of these injuries occur as a side effect of either a tumor-treating therapy or a healing-enhancement physical therapy.

Lightning Injury

Victims of lightning injury usually manifest fern-like patterns of burn injury that are mostly confined to the outer layers of the skin, along with neuromuscular dysfunction (3, 98–100). The seriousness of a lightning strike should not be judged

by the superficial surface burns that occur on the skin. The durations of the primary pulse of lightning current and its induced secondary electrical currents are so brief that heating is typically not found in subcutaneous tissue; rather the injury appears to be a pure electrical phenomenon. As previously described, there are some exceptions to this, such as when lightning strikes and charges up a car or truck to which a victim is in contact, in which case the electrical discharge of the car or truck through the victim takes long enough for heating and burning to occur in addition to the damage from electrical effects.

Transient nerve dysfunction can have a variable course of recovery, depending on the severity of field exposure. Nerves can regain function in hours or require months. The mechanism of recovery is unknown. Permanent sequelae have been correlated with demonstrable anatomical lesions (101). Andrews et al (3) have categorized lightning strike victims in three groups of severity. (*a*) The first group are those with mild injury, in which the effects are transient. The victim is stunned by shock, may have fallen, and has been fully alert but slightly disoriented and amnesic from the event. Memory of the event is impaired for hours to days. There may also be temporary blindness and deafness. The patient may be hypertensive or hypotensive as a result of a loss of autonomic control. Recovery is gradual but usually complete. (*b*) The second moderately injured group of victims are disoriented, combative, and may manifest seizure activity. They have keraunoparalysis, which persists for several hours. Vascular spasms lead to cold, mottled, cyanotic skin over the affected distal extremities. Characteristically, these victims have superficial thermal injury to the skin, but occasionally their burns are deeper. Myocardial infarction may have occurred or might occur later, in response to the stress (102). These patients generally survive (103, 104) with permanent neurophysiologic disturbances such as paresthesias, loss of cutaneous sensation, sleep disorders, etc. (*c*) The third, severely injured group of victims have lesions in the central nervous system (100) and/or suffer myocardial infarction (98, 99). Prolonged circulatory arrest adds hypoxia/reperfusion injury to the brain. Although, survival is possible, rehabilitation potential is small.

Radiation Injury

Ionizing UV light can penetrate only the very thinnest layer of skin. Soft X-rays with wavelengths below 10 nm ($>$124 eV) have a very shallow penetration into the tissue. Radiation with energies between 12.4 and 124 keV (0.1–0.01 nm) is widely used for diagnostic purposes. It penetrates through the body, but energy deposition is so low that it can be used only for superficial therapies. Both of these X-ray classes can be produced by X-ray tubes. Deep-therapy X-rays, which are used in cancer treatments, have energies of $>$124 keV and are typically produced in linear accelerators. These radiation beams easily penetrate the entire body and produce damage along their travel pathway. To optimize cancer treatment effects with a minimum of damage in noncancerous tissue, cancer therapies therefore use multiple beams that intersect at the center of the tumor.

Annu. Rev. Biomed. Eng. 2000.2:477-509. Downloaded from arjournals.annualreviews.org
by UNIVERSITY OF CHICAGO LIBRARIES on 10/02/06. For personal use only.

Immediately after an exposure to intense irradiation, no visible changes are manifested. In irradiated areas, skin wounds develop as cells lose their ability to proliferate or produce extracellular matrix. All irradiated cells are affected. Tissue breakdown ensues as widespread edema and inflammation occur, as a result of the loss of capillary function. At radiation doses of >80–100 Gy, even postmitotic cells are killed via extensive lipid peroxidation and resultant bilayer membrane permeabilization (87). In nerve cells, this leads to central nervous system arrest, which in turn leads to death within hours of exposure. The clinical syndrome resulting from this massive exposure is called the neurologic syndrome (105).

Annu. Rev. Biomed. Eng. 2000.2:477-509. Downloaded from arjournals.annualreviews.org
by UNIVERSITY OF CHICAGO LIBRARIES on 10/02/06. For personal use only.

SUMMARY AND CONCLUSIONS

Given the importance of electrical power to human culture, the problem of electrical injury is one that will continue to exist for the foreseeable future. Electrical injury has been poorly understood and perhaps less than optimally managed in the past. Improvement requires a better understanding of injury mechanisms, anatomical patterns of injury, and therapy. A prompt, accurate clinical diagnosis of electrical injury is one of the most difficult tasks in the medical field (5) because it usually calls for an understanding of the interaction between electric current and human tissue. Specifically, the difficulty involves the following:

1. The exact tissue damage mechanism and damage level depend on a host of parameters: the characteristics of the power source (dc or ac current, voltage, frequency, etc), path and duration of closed circuit, area and impedance of contact spot, etc. Correspondingly, there is a whole spectrum of damage characteristics that depend on the values of these parameters. The physician needs to do four-dimensional (spatial plus temporal) detective work to arrive at a correct diagnosis.
2. Electrical damage to the tissues is not easily detectable by visual inspection or physical examination, and often its sequelae will not manifest themselves until after a certain period of time; for instance, electrically injured tissue may initially appear viable, only to become visibly necrotic at a later point (in a number of days) (94, 106, 107).

The molecular structure of biological systems can be severely altered by the effects of high-energy, commercial-frequency electrical power. The mechanisms of damage include cell membrane electroporation, Joule heating, electroconformational protein denaturation, and others.

ACKNOWLEDGMENTS

Parts of the research presented were funded by grants from the Electric Power Research Institute (RP WO-2914 and RP WO-9038), the National Institutes of Health (NIGMS 5-R01 GM53113), and Commonwealth Edison.

Visit the Annual Reviews home page at www.AnnualReviews.org

LITERATURE CITED

1. Occupational Safety & Health Administration. 1999. Statistics & Data. US Dep. Labor. http://www.osha.gov/oshstats
2. Gourbiere E. 1992. Work-related electrical burns. Presented at *Proc. Ann. Int. Conf. IEEE Eng. Med. Biol. Soc., Nov. 14th, Paris*. Piscataway, NJ: Inst. Elect. Electron. Eng.
3. Andrews CJ, Cooper MA, Darveniza M, Mackerras D. 1992. *Lightning Injuries: Electrical, Medical, and Legal Aspects*. Boca Raton, FL: CRC Press. 195 pp.
4. *Accident Facts: 1983*. 1983. National Safety Council. Chicago, IL
5. Lee RC. 1997. Injury by electrical forces: pathophysiology, manifestations, and therapy. *Curr. Probl. Surg.* 34(9):677–75
6. Hunt JL. 1992. Soft tissue patterns in acute electrical burns. In *Electrical Trauma: The Pathophysiology, Manifestations, and Clinical Management*, ed. RC Lee, EG Cravalho, JF Burke, pp. 83–104. Cambridge, UK: Cambridge Univ. Press
7. Dalziel CF. 1943. Effect of frequency on let-go currents. *Trans. Am. Inst. Electr. Eng.* 62:745–50
8. Dalziel CF, Lee WR. 1969. Lethal electric currents. *IEEE Spectrum* 6:44–50
9. Duling BR. 1983. The kidney. In *Physiology*, ed. RM Berne, MN Levy, pp. 821–92. St. Louis, MO: Mosby. 1165 pp.
10. Geddes LA, Baker LE. 1967. The specific resistance of biological material: a compendium of data for the biomedical engineer and physiologist. *Med. Biol. Eng.* 5:271–93
11. Lee RC, Kolodney MS. 1987. Electrical injury mechanisms: dynamics of the thermal response. *Plast. Reconstr. Surg.* 80:663–71
12. Daniel RK, Ballard PA, Heroux P, Zelt RG, Howard CR. 1988. High–voltage electrical injury—acute patho-physiology. *J. Hand Surg. Am.* 13(1):44–49
13. Sances A, Myklebust JB, Larson SJ, Darin JC, Swiontek T, et al. 1981. Experimental electrical injury studies. *J. Trauma* 21(8):589–97
14. Gaylor DG, Prakah-Asante A, Lee RC. 1988. Significance of cell size and tissue structure in electrical trauma. *J. Theor. Biol.* 133:223–37
15. Bhatt DL, Gaylor DC, Lee RC. 1990. Rhabdomyolysis due to pulsed electric fields. *Plast. Reconstr. Surg.* 86(1):1–11
16. Block TA, Aarsvold JN, Matthews KL II, Mintzer RA, River LP, et al. 1995. Nonthermally mediated muscle injury and necrosis in electrical trauma. *J. Burn Care Rehabil.* 16(6):581–88
17. Lee RC, Astumian RD. 1996. The physicochemical basis for thermal and nonthermal "burn" injury. *Burns* 22(7):509–19
18. Capelli-Schellpfeffer M, Lee RC, Toner M, Diller KR. 1998. Correlation between electrical accident parameters and injury. *IEEE Ind. Appl. Mag.* 4(2):25–31
19. Parsegian A. 1969. Energy of an ion crossing a low dielectric membrane: solutions to four relevant problems. *Nature* 221:844–46
20. Mandel LJ. 1987. Bioenergetic of membrane processes. In *Membrane Physiology*, ed. TE Andreoli, et al, pp. 295–310. New York: Plenum Med. 2nd ed.
21. Weaver JC, Chizmadzhev YA. 1996. Theory of electroporation: a review. *Bioelectrochem. Bioenerg.* 41:135–60
22. Ho SY, Mittal GS. 1996. Electroporation of cell membranes: a review. *Crit. Rev. Biotechnol.* 16(4):349–62
23. Neumann E, Kakorin S, Tönsing K. 1999. Fundamentals of electroporative delivery of drugs and genes. *Bioelectrochem. Bioenerg.* 48:3–16
24. Cevc G. 1990. Membrane electrostatics. *Biochim. Biophys. Acta* 1031–3:311–82

Annu. Rev. Biomed. Eng. 2000.2:477-509. Downloaded from arjournals.annualreviews.org
by UNIVERSITY OF CHICAGO LIBRARIES on 10/02/06. For personal use only.

Annu. Rev. Biomed. Eng. 2000.2:477-509. Downloaded from arjournals.annualreviews.org
by UNIVERSITY OF CHICAGO LIBRARIES on 10/02/06. For personal use only.

25. Lee RC, Aarsvold JN, Chen W, Astumian RD, Capelli-Schellpfeffer M, et al. 1995. Biophysical mechanisms of cell membrane damage in electrical shock. *Semin. Neurol.* 15(4):367–74
26. Chen W, Lee RC. 1994. Altered ion channel conductance and ionic selectivity induced by large imposed membrane potential pulse. *Biophys. J.* 67(2):603–12
27. Weaver JC. 1993. Electroporation: a general phenomenon for manipulating cells and tissue. *J. Cell. Biochem.* 51:426–35
28. Teissie J, Eynard N, Gabriel B, Rols P. 1999. Electropermeabilization of cell membranes. *Adv. Drug Deliv. Rev.* 35:3–19
29. Neumann E, Sowers AE, Jordan CA, eds. 1989. *Electroporation and Electrofusion in Cell Biology*. New York: Plenum. 436 pp.
30. Chang DC, Chassy BM, Saunders JA, Sowers AE, eds. 1992. *Guide to Electroporation and Electrofusion*. New York: Academic. 581 pp.
31. Lynch PT, Davey MR, eds. 1996. *Electrical Manipulation of Cells*. New York: Chapman & Hall. 292 pp.
32. Bier M, Hammer SM, Canaday DJ, Lee RC. 1999. Kinetics of sealing for transient electropores in isolated mammalian skeletal muscle cells. *Bioelectromagnetics* 20:194–201
33. Gabriel B, Teissie J. 1997. Direct observation in the millisecond time range of fluorescent molecule asymmetrical interaction with the electropermeabilized cell membrane. *Biophys. J.* 73:2630–37
34. Gabriel B, Teissie J. 1998. Mammalian cell electropermeabilization as revealed by millisecond imaging of fluorescence changes of ethidium bromide in interaction with the membrane. *Bioelectrochem. Bioenerg.* 47:113–18
35. Gowrishankar TR, Chen W, Lee RC. 1998. Non-linear microscale alterations in membrane transport by electropermeabilization. *Ann. NY Acad. Sci.* 858:205–16
36. Chizmadzhev AY, Arakelyan VB, Pastushenko VF. 1979. Electric breakdown of bilayer membranes. III. Analysis of possible mechanisms of defect origin. *Bioelectrochem. Bioenerg.* 6:63–70
37. Glaser RW, Leikin SL, Chernomordik LV, Pastushenko VF, Sokirko AI. 1988. Reversible electrical breakdown of lipid bilayers: formation and evolution of pores. *Biochim. Biophys. Acta* 940:275–87
38. Neu JC, Krassowska W. 1999. Asymptotic model of electroporation. *Phys. Rev. E* 59(3):3471–82
39. DeBruin KA, Krassowska W. 1999. Modeling electroporation in a single cell. I. Effects of field strength and rest potential. *Biophys. J.* 77:1213–24
40. DeBruin KA, Krassowska W. 1999. Modeling electroporation in a single cell. II. Effects of ionic concentrations. *Biophys. J.* 77:1225–33
41. Hibino M, Shigemori M, Itoh H, Nagayma K, Kinosita K. 1991. Membrane conductance of an electroporated cell analyzed by submicrosecond imaging of transmembrane potential. *Biophys. J.* 59:209–20
42. Kinosita K, Hibino M, Itoh H, Shigemori M, Hirano K, et al. 1992. Events of membrane electroporation visualized on a time scale from microseconds to seconds. See Ref. 30, pp. 29–46
43. Knisley SB, Grant AO. 1994. Asymmetrically electrically induced injury of rabbit ventricular myocytes. *J. Mol. Cell. Cardiol.* 27:1111–22
44. Hibino M, Itoh H, Kinosita K. 1993. Time courses of cell electroporation as revealed by submicrosecond imaging of transmembrane potential. *Biophys. J.* 64:1789–1800
45. Neumann E, Sprafke A, Boldt E, Wolff H. 1992. Biophysical considerations of membrane electroporation. See Ref. 30, pp. 77–90
46. Rols MP, Teissie J. 1990. Electropermeabilization of mammalian cells: quantitative analysis of the phenomenon. *Biophys. J.* 58:1089–98
47. Lee RC, Gaylor DC, Prakah-Asante K,

Annu. Rev. Biomed. Eng. 2000.2:477-509. Downloaded from arjournals.annualreviews.org
by UNIVERSITY OF CHICAGO LIBRARIES on 10/02/06. For personal use only.

Bhatt D, Israel DA. 1988. Role of cell membrane rupture in the pathogenesis of electrical trauma. *J. Surg. Res.* 44(6):709–19

48. Gaylor DC, Lee RC. 1992. Skeletal muscle cell membrane electrical breakdown in electrical trauma. See Ref. 6, pp. 401–25
49. Tung L. 1992. Electrical injury to heart muscle cells. See Ref. 6, pp. 361–400
50. Tung L, Tovar O, Neunlist M, Jain SK, O'Neill RJ. 1994. Effects of strong electrical shock on cardiac muscle tissue. *Ann. NY Acad. Sci.* 720:160–75
51. Mir LM, Glass LF, Sersa G, Teissie J, Domenge C, et al. 1998. Effective treatment of cutaneous and subcutaneous malignant tumours by electrochemotherapy. *Br. J. Cancer* 77(12):2336–42
52. Heller R, Jaroszeski MJ, Reintgen DS, Puleo CA, DeConti RC, et al. 1998. Treatment of tumors with electrochemotherapy using intralesional bleomycin. *Cancer* 83:148–57
53. Aihara H, Miyazaki JI. 1998. Gene transfer into muscle by electroporation *in vivo*. *Nat. Biotechnol.* 16:867–70
54. Mir LM, Bureau MF, Gehl J, Rangara R, Rouy D, et al. 1999. High-efficiency gene transfer into skeletal muscle mediated by electric pulses. *Proc. Natl. Acad. Sci. USA* 96:4262–67
55. Pliquett U, Langer R, Weaver JC. 1995. Changes in the passive electrical properties of human stratum corneum due to electroporation. *Biochim. Biophys. Acta* 1239:111–21
56. Prausnitz MR, Lee CS, Liu CH, Pang JC, Singh TP, et al. 1996. Transdermal transport efficiency during skin electroporation and iontophoresis. *J. Control. Release* 38:205–17
57. *Adv. Drug Delivery Rev.* 1999. 35(1):1–137
58. Tropea BI, Lee RC. 1992. Thermal injury kinetics in electrical trauma. *J. Biomech. Eng.* 114(2):241–50
59. Diller KR. The mechanisms and kinetics of heat injury accumulation. *Ann. NY Acad. Sci.* 720:38–55
60. Reilly JP. 1994. Scales of reaction to electric shock: thresholds and biophysical mechanisms. *Ann. NY Acad. Sci.* 720:21–37
61. DeBono R. 1999. A histological analysis of a high voltage electric current injury to an upper limb. *Burns* 50:541–47
62. Shen AC, Jennings KB. 1972. Kinetics of calcium accumulation in acute myocardial ischemic injury. *Am. J. Pathol.* 67:441–52
63. Matthews KL II, 1997. *Development and application of a small gamma camera*. PhD thesis. Univ. Chicago, Chicago, Ill. 142 pp.
64. Eyring H, Lin SH, Lin SM. 1980. *Basic Chemical Kinetics*. New York: Wiley Intersci. 493 pp.
65. Moussa NA, McGrath JJ, Cravalho EG, Asimacopoulos PJ. 1977. Kinetics of thermal injury in cells. *J. Biomed. Eng.* 99:155–59
66. Rocchio CM. 1989. *The kinetics of thermal damage to an isolated skeletal muscle cell*. SB thesis. MIT, Cambridge, MA.
67. Cravalho EG, Toner M, Gaylor D, Lee RC. 1992. Response of cells to supraphysiologic temperatures: experimental measurements and kinetic models. See Ref. 6, pp. 281–300
68. Henriques FC. 1947. Studies in thermal injuries V: the predictability and the significance of thermally induced rate processes leading to irreversible epidermal damage. *Arch. Pathol.* 43:489–502
69. Henriques FC, Moritz AR. 1944. Studies in thermal injuries. I. The conduction of heat to and through skin and the temperature attained therein. *Am. J. Pathol.* 23:531–49
70. Gershfeld NL, Murayama M. 1968. Thermal instability of red blood cell membrane bilayers: temperature dependence of hemolysis. *J. Membr. Biol.* 101:62–72
71. Moussa NA, Tell EN, Cravalho EG. 1979. Time progression of hemolysis of erythrocyte populations exposed to supraphysiologic temperatures. *J. Biomech. Eng.* 101:213–17
72. Gaylor D. 1989. *Role of electromechanical*

Annu. Rev. Biomed. Eng. 2000.2:477-509. Downloaded from arjournals.annualreviews.org
by UNIVERSITY OF CHICAGO LIBRARIES on 10/02/06. For personal use only.

instabilities in electroporation of cell membranes. PhD thesis. MIT, Cambridge, MA. 165 pp.

73. Merchant FA, Holmes WH, Capelli-Schellpfeffer M, Lee RC, Toner M. 1998. Poloxamer 188 enhances functional recovery of lethally heat-shocked fibroblasts. *J. Surg. Res.* 74:131–40
74. Bischof JC, Padanilam J, Holmes WH, Ezzell RM, Lee RC, et al. 1995. Dynamics of cell membrane permeability changes at supraphysiological temperatures. *Biophys. J.* 68(8):2608–14
75. Tsong TY, Astumian RD. 1987. Electroconformational coupling and membrane protein function. *Prog. Biophys. Mol. Biol.* 50:1–45
76. Chen W, Lee RC. 1994. Altered ion channel conductance and ionic selectivity induced by large imposed membrane potential pulse. *Biophys. J.* 67:603–12
77. Chen W, Han Y, Chen Y, Astumian RD. 1998. Electric field-induced functional reductions in the K+ channels mainly resulted from supramembrane potential-mediated electroconformational changes. *Biophys. J.* 75(1):196–206
78. Chou CK. 1995. Radiofrequency hyperthermia in cancer therapy. In *The Biomedical Engineering Handbook*, ed. JD Bronzino, pp. 1424–30. Boca Raton, FL: CRC Press
79. Sneed PK, Gutin PH, Stauffer P. 1992. Thermoradiotherapy of recurrent malignant brain tumors. *Int. J. Radiat. Oncol. Biol. Phys.* 23(4):853–61
80. van Rhoon GC, van der Zee J, Broekmeyer-Reurink MP, Visser AG, Reinhold HS. 1992. Radiofrequency capacitive heating of deep-seated tumours using pre-cooling of the subcutaneous tissues: results on thermometry in Dutch patients. *Int. J. Hyperth.* 8(6):843–54
81. Nicholson CP, Grotting JC, Dimick AR. 1987. Acute microwave injury to the hand. *J. Hand Surg. Am.* 12(3):446–49
82. Alexander RC, Surrell JA, Cohle SD. 1987. Microwave oven burns to children: an unusual manifestation of child abuse. *Pediatrics* 79(2):255–60
83. Surrell JA, Alexander RC, Cohle SD, Lovell FR Jr, Wehrenberg RA. Effects of microwave radiation on living tissues. *J. Trauma* 27(8):935–39
84. Harm W. 1980. *Biological Effects of Ultraviolet Radiation*. Cambridge, MA: Cambridge Univ. Press. 216 pp.
85. Pizzagrello DJ, Witcofski RL. 1967. *Basic Radiation Biology*. Malvern, PA: Lea & Febiger. 301 pp.
86. Halliwell B, Gutteridge J, eds. 1989. *Free Radicals in Biology and Medicine*. Oxford, UK: Clarendon. 543 pp. 2nd ed.
87. Canaday D, Li P, Weichselbaum R, Astumian RD, Lee RC. Membrane permeability changes in gamma-irradiated muscle cells. *Ann. NY Acad. Sci.* 720:153–59
88. Peterson RR. 1980. *A Cross-Sectional Approach to Anatomy*. Chicago: Yearbook Med.
89. Freiberger H. 1933. The electrical resistance of the human body to commercial direct and alternating *currents*. *Elektr. wirtsch.* 32(2):442–46; 32(17):373–75. (In German)
90. Pennes HH. 1948. Analysis of tissue and arterial blood temperatures in the resting human forearm. *J. Appl. Physiol.* pp. 93–122
91. Jones RA, Liggett DP, Capelli-Schellpfeffer M, Macaladay T, Saunders LF, et al. 1997. Staged tests increase awareness of arc-flash hazards in electrical equipment. *IEEE Ind. Appl. Soc. Proc. PCIC*, 313–22 (Abstr.)
92. Hannig J, Kovar DA, Abramov GS, Zhang D, Zamora M, et al. 1999. Contrast enhanced MRI of electroporation injury. *Proc. Jt. BMES/EMBS Conf., 1st*, CD 1078 (Abstr.)
93. Kovar DA, Lewis MZ, River JN, Lipton MJ, Karczmar GS. 1997. In vivo imaging of extraction fraction of low molecular weight MR contrast agents and perfusion

rate in rodent tumors. *Magn. Reson. Med.* 38:259–68
94. Baxter CR. 1970. Present concepts in the management of major electrical injury. *Surg. Clin. North. Am.* 50:1401–18
95. Hunt JL, Sato RM, Baxter CR. 1980. Acute electric burns: current diagnostic and therapeutic approaches to management. *Arch. Surg.* 115:434
96. Zelt RG, Ballard PA, Common AA, et al. 1986. Experimental high voltage electrical burns: the role of progressive necrosis. *Surg. Forum* 37:624–26
97. Isager P, Lind T. 1995. Accidental third-degree burn caused by bipolar electrocoagulation. *Injury* 26(5):357
98. Sinha AK. 1985. Lightning induced myocardial injury—a case report with management. *Angiology* 36(5):327–31
99. Cooper MA. 1980. Lightning injuries: prognostic signs for death. *Ann. Emerg. Med.* 9:134–38
100. Ravitch MM, Lane R, Safar P, Steichen FM, Knowles P. 1961. Lightning stroke. *N. Engl. J. Med.* 264:36–38
101. Hooshimand HF, Radfar F, Beckner E. 1989. The neurophysiological aspects of electrical injuries. *Electroencephalogy* 20:111–20
102. Moran KT, Thupari JN, Munster AM. 1986. Electric and lightning induced cardiac arrest reversed by prompt cardiopulmonary resuscitation. *JAMA* 255:211–57
103. Amy BW, McManus WF, Goodwin CW, Pruitt BA. 1985. Lightning injury with survival in five patients. *JAMA* 253:243–45
104. Taussig HA. 1968. "Death" from lightning—and the possibility of living again. *Ann. Intern. Med.* 68(6):1345–53
105. Nias AHW. 1998. *An Introduction to Radiobiology*, pp. 241–57. New York: Wiley & Sons. 384 pp. 2nd ed.
106. Artz CP. 1967. Electrical injury simulated crush injury. *Surg. Gynecol. Obstet.* 125:1316–17
107. Hammond J, Ward CG. 1994. The use of Tc99m-PYP scanning in management of high-voltage electrical injuries. *Am. Surg.* 60:886–88

Annu. Rev. Biomed. Eng. 2000.2:477-509. Downloaded from arjournals.annualreviews.org
by UNIVERSITY OF CHICAGO LIBRARIES on 10/02/06. For personal use only.

Annu. Rev. Biomed. Eng. 2000.2:477-509. Downloaded from arjournals.annualreviews.org
by UNIVERSITY OF CHICAGO LIBRARIES on 10/02/06. For personal use only.

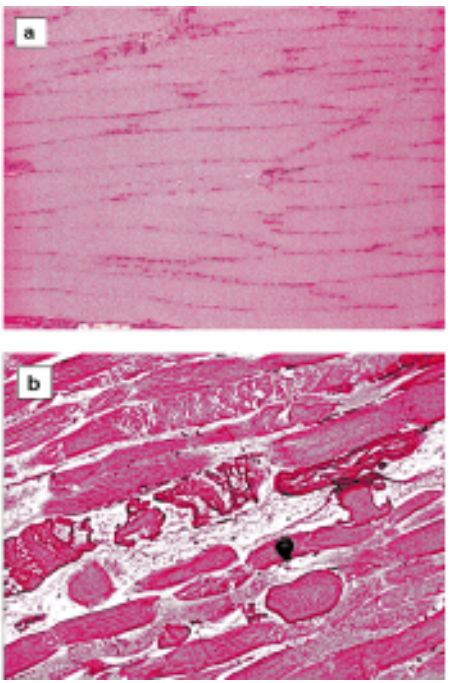

Figure 5 Longitudinal histology sections of skeletal muscle tissue subjected to nine 4-ms dc-pulses with 2 A,150 Vcm^{-1} (*b*) compared with nonshocked control (*a*). Sections were stained with hematoxylin/eosin and show muscle cell damage in the form of extensive vacuolization and hypercontraction band degeneration; biopsy was taken at 6 h post-shock.

Annual Review of Biomedical Engineering
Volume 2, 2000

CONTENTS

Annu. Rev. Biomed. Eng. 2000.2:477-509. Downloaded from arjournals.annualreviews.org
by UNIVERSITY OF CHICAGO LIBRARIES on 10/02/06. For personal use only.

Annu. Rev. Biomed. Eng. 2000.2:477-509. Downloaded from arjournals.annualreviews.org
by UNIVERSITY OF CHICAGO LIBRARIES on 10/02/06. For personal use only.